Mon. Not. R. Astron. Soc. **353,** 500–510 (2004) doi:10.1111/j.1365-2966.2004.08084.x

Cosmic star formation: constraints on the galaxy formation models

F. Calura,[1⋆] F. Matteucci[1] and N. Menci[2]
[1]*Dipartimento di Astronomia–Universitá di Trieste, Via G. B. Tiepolo 11, 34131 Trieste, Italy*
[2]*INAF, Osservatorio Astronomico di Roma, via Frascati 33, I-00040 Monteporzio, Italy*

Accepted 2004 May 27. Received 2004 May 27; in original form 2004 March 19

ABSTRACT

We study the evolution of the cosmic star formation in the Universe by computing the luminosity density (in the UV, *B*, *J* and *K* bands) and the mass density of galaxies in two reference models of galaxy evolution: the pure-luminosity evolution (PLE) model developed by Calura & Matteucci and the semi-analytical model (SAM) of hierarchical galaxy formation by Menci et al. The former includes a detailed description of the chemical evolution of galaxies of different morphological types; it does not include any number evolution of galaxies whose number density is normalized to the observed local value. On the other hand, the SAM includes a strong density evolution following the formation and the merging histories of the DM haloes hosting the galaxies, as predicted by the hierarchical clustering scenario, but it does not contain morphological classification or chemical evolution. Our results suggest that at low–intermediate redshifts ($z < 1.5$) both models are consistent with the available data on the luminosity density of galaxies in all the considered bands. At high redshift the luminosity densities predicted in the PLE model show a peak due to the formation of ellipticals, whereas in the hierarchical picture a gradual decrease of the star formation and of the luminosity densities is predicted for $z > 2.5$. At such redshifts the PLE predictions tend to overestimate the present data in the *B* band, whereas the SAM tends to underestimate the observed UV luminosity density. As for the stellar mass density, the PLE picture predicts that nearly 50 and 85 per cent of the present stellar mass is in place at $z \sim 4$ and $z \sim 1$, respectively. According to the hierarchical SAM, 50 and 60 per cent of the present stellar mass is completed at $z \sim 1.2$ and $z = 1$, respectively. Both predictions fit the observed stellar mass density evolution up to $z = 1$. At $z > 1$, the PLE model and SAM tend to overestimate and underestimate the observed values, respectively. We discuss the origin of the similarities and of the discrepancies between the two models, and the role of observational uncertainties (such as dust extinction) in comparing models with observations.

Key words: galaxies: evolution – galaxies: formation – galaxies: fundamental parameters.

1 INTRODUCTION

In the past few years a great deal of work has appeared on the subject of galaxy formation and evolution. With the word 'formation' usually one means the assembly of the bulk of the material (say >50 per cent) of the luminous part of a galaxy, namely the stars and the gas, within a sphere of radius ∼30 kpc (Peebles 2002). A reliable picture of galaxy formation must be able to reproduce, at the same time, all (or as much as possible) of the available constraints, including colours and chemical abundances. Currently, the most intriguing debate on galaxy evolution concerns how the formation of ellipticals and bulges occurred in the Universe. In fact, the two main competing scenarios of galaxy evolution propose rather different conditions for the formation of spheroids. In the first scenario, ellipticals and bulges formed at high redshift (e.g. $z > 2$–3) as the result of a violent burst of star formation following a 'monolithic collapse' (MC) of a gas cloud. After the main burst of star formation, the galaxy lost the residual gas by means of a galactic wind and it has evolved passively since then (Larson 1974; van Albada 1982; Sandage 1986; Matteucci & Tornambé 1987; Arimoto & Yoshii 1987; Matteucci 1994). The MC view, or better, the idea that spheroids formed quickly and at high redshift, is supported by a large set of observational evidence. Among this set, of particular importance are the thinness of the fundamental plane (Djorgovski & Davis 1987; Renzini & Ciotti 1993; Bernardi et al. 1998; Kochanek et al. 2000; van Dokkum et al. 2001; Rusin et al. 2003; van Dokkum & Ellis 2003), the overabundance of Mg relative to Fe observed in the stars as well as the increase of the [Mg/Fe] ratio with galaxy luminosity (Pipino & Matteucci 2004, and references therein), and

⋆E-mail: fcalura@ts.astro.it

the tightness of the colour–central velocity dispersion and colour–magnitude relations (Bower, Lucey & Ellis 1992; Kodama, Bower & Bell 1999) observed for both cluster and field spheroids at high and low redshift, as well as the constancy of the number density of both spheroids and large discs observed up to $z \sim 1$ (Im et al. 1996; Lilly et al. 1998; Schade et al. 1999; Im et al. 2002).

On the other hand, the hierarchical clustering (HC) picture is based on the Press & Schechter (1974) structure formation theory, which has been developed mainly to study the behaviour of the dark matter (DM). According to this theory, in a Λ cold dark matter (ΛCDM)-dominated universe, small DM haloes are the first to collapse, then interact and merge to form larger haloes. The most uncertain assumption in the HC scenario concerns the behaviour of the baryonic matter, which is assumed to follow the DM in all the interaction and merging processes. In this framework, massive spheroids are formed from several merging episodes among gas-rich galaxies, such as discs, occurring throughout the whole Hubble time. These mergers produce moderate star formation rates (SFRs), with massive galaxies reaching their final masses at more recent epochs than less massive ones ($z \leqslant 1.5$: White & Rees 1978 ; Kauffmann, White & Guiderdoni 1993; Baugh et al. 1998; Cole et al. 2000; Somerville, Primack & Faber 2001; Menci et al. 2002). The observational evidence in favour of hierarchical galaxy formation is the apparent paucity of giant galaxies at high redshift ($z \sim 1$) as claimed by some authors (Kauffmann, Charlot & White 1996; Zepf 1997; Barger et al. 1999), and the blue colours of some spheroids at low redshift, possibly ascribed to residual star formation activity induced by mergers (Franceschini et al. 1998; Menanteau et al. 1999), as well as observations showing evidence for mergers in distant field and cluster galaxies (van Dokkum et al. 2000; Bundy et al. 2004) and the increase of the measured merging rate with redshift (Patton et al. 1997; Le Févre et al. 2000; Conselice et al. 2003).

Recently, Calura & Matteucci (2003, hereinafter CM03) have developed a series of detailed chemical and spectrophotometric models for elliptical, spiral and irregular galaxies, used to study the evolution of the luminous matter in the Universe and the contributions that galaxies of different morphological types bring to the overall cosmic star formation. It is worth noting that all these models reproduce the chemical abundances and abundance patterns in the aforementioned galaxies.

In their scenario of pure luminosity evolution (PLE), only the galaxy luminosities evolve, whereas the number densities are assumed to be constant and equal to the values indicated by the local *B*-band luminosity function (LF), as observed by Marzke et al. (1998). In this paper, we compare the cosmic star formation history as predicted by the PLE model of CM03 with the predictions of the hierarchical semianalytic model (SAM) developed by Menci et al. (2002). We want to stress that the PLE model and the SAM do not represent the only alternatives to study galaxy evolution. For instance, several groups have studied the evolution of the cosmic star formation by means of large-scale hydrodynamical simulations (e.g. Springel & Hernquist 2003; Nagamine et al. 2004), which are generally based on the ΛCDM cosmological model. Furthermore, we want to stress that the two scenarios are not necessarily in contradiction, since HC was devised for the DM whereas PLE was devised for the baryonic matter. As some observational evidence seems to indicate, it is in fact possible that, although DM halo formation is hierarchical, the baryonic matter evolved in an anti-hierarchical fashion, in the sense that larger galaxies are older than small ones (Matteucci 1994; Pipino & Matteucci 2004). By comparing the model predictions with a large set of observational data, we aim to infer whether the two main competing scenarios can be disentangled on the basis of the current observations. The novelty with respect to the paper by CM03 is the incorporation of dust extinction in the PLE model, with important consequences for the predicted behaviour of the luminosity of galaxies at short wavelengths, i.e. in the UV and *B* photometric bands. This paper is organized as follows. In Sections 2 and 3, we describe the PLE model as developed by CM03 and the SAM developed by Menci et al. (2002), respectively. In Section 4 we present our results, and in Section 5 we draw the conclusions. Unless otherwise stated, throughout the paper we use a ΛCDM cosmological model characterized by $\Omega_0 = 0.3$, $\Omega_\Lambda = 0.7$ and $h = 0.65$.

2 THE CM03 PURE LUMINOSITY EVOLUTION MODEL

The PLE models developed by CM03 consist of chemical evolution models for galaxies of different morphological types (ellipticals, spirals, irregulars), used to calculate metal abundances and SFRs, and a spectrophotometric code used to calculate galaxy spectra, colours and magnitudes by taking into account the chemical evolution. Detailed descriptions of the chemical evolution models for galaxies of different morphological types can be found in Matteucci & Tornambé (1987) and Matteucci (1994) for elliptical galaxies, Chiappini, Matteucci & Gratton (1997) and Chiappini, Matteucci & Romano (2001) for the spirals, and Bradamante, Matteucci & D'Ercole (1998) for irregular galaxies. We assume that the category of galactic bulges is naturally included in that of elliptical galaxies. Our assumption is supported by the similar features characterizing bulges and ellipticals: for instance, both are dominated by old stellar populations and respect the same fundamental plane (Binney & Merrifield 1998; Renzini 1999). This indicates that they are likely to have a common origin, i.e. both are likely to have formed on very short time-scales and a long time ago, and we will refer to both ellipticals and bulges as the 'spheroids'.

In our picture, spheroids form as a result of the rapid collapse of a homogeneous sphere of primordial gas where star formation is taking place at the same time as the collapse proceeds. Star formation is assumed to halt as the thermal energy of the interstellar medium (ISM), heated by stellar winds and supernova (SN) explosions, balances the binding energy of the gas. At this time a galactic wind occurs, sweeping away almost all of the residual gas. By means of the galactic wind, ellipticals enrich the intergalactic medium (IGM) with metals.

For spiral galaxies, the adopted model is calibrated in order to reproduce a large set of observational constraints for the Milky Way galaxy (Chiappini et al. 2001). The Galactic disc is approximated by several independent rings, 2 kpc wide, without exchange of matter between them. In our picture, spiral galaxies are assumed to form as a result of two main infall episodes. During the first episode, the halo and the thick disc are formed. During the second episode, a slower infall of external gas forms the thin disc with the gas accumulating faster in the inner than in the outer region ('inside-out' scenario: Matteucci & François 1989). The process of disc formation is much longer than the halo and bulge formation, with time-scales varying from $\sim$2 Gyr in the inner disc to $\sim$8 Gyr in the solar region and up to 10–15 Gyr in the outer disc.

In this case, at variance with Chiappini et al. (2001), CM03 assume a Salpeter (1955) initial mass function (IMF), instead of the Scalo (1986) IMF. This choice is motivated by the fact that Scalo and Salpeter IMFs in spirals produce very similar results in the study of

the luminosity density evolution, and also by the fact that we aim to test the hypothesis of a universal IMF (see also Calura & Matteucci 2004). Another difference between the Chiappini et al. (2001) model and ours concerns the elimination of the star formation threshold, motivated by the fact that its effects are appreciable only on small scales, i.e. in the chemical evolution of the solar vicinity and of small galactic regions, whereas our aim is to study star formation in galactic discs on global scales.

Finally, irregular dwarf galaxies are assumed to assemble from continuous infall of gas of primordial chemical composition, until masses in the range $\sim 10^8$ –6×10^9 $M_\odot$ are accumulated, and to produce stars at a lower rate than spirals.

Let G_i be the fractional mass of the element i in the gas within a galaxy; its temporal evolution is described by the basic equation

$$\dot{G}_i = -\psi(t) X_i(t) + R_i(t) + (\dot{G}_i)_{\rm inf} - (\dot{G}_i)_{\rm out}, \quad (1)$$

where $G_i(t) = \sigma_{\rm g}(t) X_i(t)/\sigma_{\rm tot}$ is the gas mass in the form of an element i normalized to a total initial mass $M_{\rm tot}$. The quantity $X_i(t) = G_i(t)/G(t)$ represents the abundance in mass of an element i, with the summation over all elements in the gas mixture being equal to unity. The quantity $G(t) = \sigma_{\rm g}(t)/\sigma_{\rm tot}$ is the fractional mass of gas present in the galaxy at time t. $\psi(t)$ is the instantaneous SFR, namely the fractional amount of gas turning into stars per unit time; $R_i(t)$ represents the returned fraction of matter in the form of an element i that the stars eject into the ISM through stellar winds and SN explosions; this term contains all the prescriptions regarding the stellar yields and the SN progenitor models. The two terms $(\dot{G}_i)_{\rm inf}$ and $(\dot{G}_i)_{\rm out}$ account for the infalling external gas from the IGM and for the outflow, occurring by means of SN-driven galactic winds, respectively. The main feature characterizing a particular morphological galactic type is represented by the prescription adopted for the star formation history.

In the case of elliptical and irregular galaxies the SFR $\psi(t)$ (in $\rm Gyr^{-1}$) has a simple form and is given by

$$\psi(t) = \nu G(t). \quad (2)$$

The quantity ν is the efficiency of star formation, namely the inverse of the typical time-scale for star formation, and for ellipticals and bulges is assumed to be $\sim$10–15 $\rm Gyr^{-1}$ (Matteucci 1994). In the case of spheroids, ν is assumed to drop to zero at the onset of a galactic wind, which develops as the thermal energy of the gas heated by SN explosions exceeds the binding energy of the gas (Arimoto & Yoshii 1987; Matteucci & Tornambé 1987). This quantity is strongly influenced by assumptions concerning the presence and distribution of DM (Matteucci 1992); for the model adopted here a diffuse ($R_{\rm e}/R_{\rm d} = 0.1$, where $R_{\rm e}$ is the effective radius of the galaxy and $R_{\rm d}$ is the radius of the DM core) but massive ($M_{\rm dark}/M_{\rm Lum} = 10$) dark halo has been assumed.

In the case of irregular galaxies we have assumed a continuous SFR always expressed as in (2), but characterized by an efficiency lower than the one adopted for ellipticals, i.e. $\nu = 0.01$ $\rm Gyr^{-1}$.

In the case of spiral galaxies, the SFR expression is

$$\psi(r,t) = \nu \sigma_{\rm tot}^{k_1}(r,t) \sigma_{\rm g}^{k_2}(r,t), \quad (3)$$

where $k_1 = 0.5$ and $k_2 = 1.5$ (see Matteucci & François 1989; Chiappini et al. 1997). For massive stars ($M > 8$ $M_\odot$) we adopt nucleosynthesis prescriptions by Nomoto et al. (1997a), the yields by van den Hoeck & Groenwegen (1997) for low- and intermediate-mass stars ($0.8 \leqslant M/M_\odot \leqslant 8$) and those of Nomoto et al. (1997b) for Type Ia SNe.

For all galaxies, we assume a Salpeter IMF, expressed by the formula

$$\phi(m) = \phi_0 m^{-(1+x)} \quad (4)$$

with $x = 1.35$, the mass range being $0.1 \leqslant m/M_\odot \leqslant 100$.

To calculate galaxy colours and magnitudes, we use the photometric code by Bruzual & Charlot (2003, hereinafter BC). However, we have implemented the BC code by taking into account the evolution of metallicity in galaxies (Calura 2004). Dust extinction is also properly taken into account. The chosen geometrical dust distribution plays an important role in the modelling of dust attenuation in galaxies: usually, the 'screen' and 'slab' dust distributions represent the two most extreme cases. In the screen model, the dust is distributed along the line of sight of the stars, whereas in the slab model the dust has the same distribution as stars. The main difference between the screen and slab dust distributions is the expression of the attenuation factor, which in the former case is given by

$$a_{\rm screen} = \exp[-\tau(\lambda)], \quad (5)$$

whereas in the latter case it is given by

$$a_{\rm slab} = \{1 - \exp[-\tau(\lambda)]\}/\tau(\lambda) \quad (6)$$

(Totani & Yoshii 2000), where $\tau(\lambda)$ is the optical depth of the dust. In this case, we adopt the 'screen' geometric distribution which, according to UV and optical observations of local starburst galaxies, is to be considered favoured over the 'slab' model (Calzetti, Kinney & Storchi-Bergmann 1994). The absorbed flux $I_{\rm a}(\lambda)$ of a stellar population behind a screen of dust is given by:

$$I_{\rm a}(\lambda) = I_{\rm I}(\lambda) \exp[-\tau(\lambda)] \quad (7)$$

(Calzetti 2001), where $I_{\rm I}(\lambda)$ represents the intrinsic, unobscured flux at the wavelength λ.

We assume that the optical depth is proportional to the column density $N(g)$ and to the metallicity Z of the gas, according to

$$\tau(\lambda) = C k(\lambda) N(g) Z, \quad (8)$$

where $k(\lambda)$ is the extinction curve. For spiral galaxies, we adopt the extinction curve derived by Seaton (1979) for the Milky Way (MW) galaxy. Such a choice is motivated by the fact that we assume that, as far as the chemical and photometric features are concerned, the MW galaxy represents an average spiral. Local starburst galaxies are generally characterized by extinction curves slightly different from the ones of the MW (Calzetti 1997, 2001) and are better modelled by the expression found by Calzetti (1997). We assume that in the starbursts occurring in elliptical and irregular galaxies, the dust follows an attenuation law similar to the one estimated by Calzetti (1997) for local starbursts. The constant C in equation (8) is chosen in order to reproduce the MW average V-band extinction of $A_V = 0.17$ (Schlegel, Finkbeiner & Davis 1998).

The galaxy densities of the various morphological types are normalized according to the local B-band luminosity function observed by Marzke et al. (1998). A scenario of PLE has been assumed, namely that galaxies evolve only in luminosity and not in number. This is equivalent to assuming that the effects of galaxy interactions and mergers are negligible at any redshift. Such a picture can account for many observables, such as the evolution of the galaxy luminosity density in various bands and the cosmic SN rates (CM03). At redshifts larger than zero the absolute magnitudes are calculated according to

$$M_B(z) = M_B(z=0) + 2.5 \log \left[\frac{\int E_{\lambda/1+z}(z) R_B(\lambda)\, {\rm d}\lambda}{\int E_{\lambda/1+z}(0) R_B(\lambda)\, {\rm d}\lambda} \right], \quad (9)$$

where $M_B(z=0)$ and $M_B(z)$ are the absolute blue magnitudes at redshift 0 and z, respectively, $E_\lambda(z)\ \mathrm{d}\lambda$ is the energy per unit time radiated at the rest-frame wavelength λ by the galaxy at redshift z, and $R_B(\lambda)$ is the response function of the rest-frame B band. The second term on the right-hand side of equation (7) represents the evolutionary correction (EC), i.e. the difference in absolute magnitude measured in the rest frame of the galaxy at the wavelength of emission (Poggianti 1997).

For the LF, we assume a Schechter (1976) form, given by

$$\Phi(M)\,\mathrm{d}M = 0.4\ln(10)\Phi^* \mathrm{e}^{-X} X^{\alpha+1}\mathrm{d}\,M, \tag{10}$$

where $X = L/L^* = 10^{0.4(M-M^*)}$. $M^*(L^*)$ is the characteristic magnitude (luminosity) and is a function of redshift, whereas Φ^* and α are the normalization and the faint-end slope, respectively, and are assumed to be constant.

In bands other than B we assume that the LF shape is the same as in the B band and we calculate the LF in the given band (X) by transforming the absolute magnitudes according to the rest-frame galaxy colours as predicted by the spectrophotometric model:

$$M_X = M_B + (X-B)_{\mathrm{rf}} \tag{11}$$

The luminosity density (LD) per unit frequency in a given band (centred at the wavelength λ) and for the kth morphological type is

$$\rho_{\lambda,k} = \int \Phi_k(L_\lambda)\left(L_\lambda/L_\lambda^*\right)\mathrm{d}L_\lambda. \tag{12}$$

The total LD is given by the sum of the single contributions of spheroids, spirals and irregulars.

The stellar mass densities for galaxies of the kth morphological type are $\rho_{*,k}$ and are calculated as

$$\rho_{*,k} = \rho_{B,k}(M_*/L)_{B,k}, \tag{13}$$

where $\rho_{B,k}$ is the predicted B LD, whereas $(M_*/L)_{B,k}$ is the predicted stellar mass-to-light ratio for the kth galactic morphological type. All the galaxies are assumed to start forming stars at the same redshift $z_{\mathrm{f}} = 5$.

3 THE SEMI-ANALYTICAL MODEL

In semi-analytical models the galaxy mass distribution is derived from the merging histories of the host DM haloes, under the assumption that the galaxies contained in each halo coalesce into a central dominant galaxy if their dynamical friction time-scale is shorter than the halo survival time. The surviving galaxies (commonly referred to as satellite galaxies) retain their identity and continue to orbit within the halo. The histories of the DM condensations rely on a well-established framework (the extended Press & Schechter theory, EPST: see Bower 1991; Bond et al. 1991; Lacey & Cole 1993). However, the recipe concerning the galaxy fate inside the DM haloes is guided by a posteriori consistency with the outputs of high-resolution N-body simulations. The SAM includes the main dynamical processes taking place inside the host DM haloes, namely dynamical friction and binary aggregations of satellite galaxies. The evolution of the galaxy mass distribution is calculated by solving numerically a set of evolutionary equations (Poli et al. 1999).

The link between stellar evolution and the dynamics follows a procedure widely used in semi-analytic models. The baryonic content $(\Omega_{\mathrm{b}}/\Omega_{\mathrm{m}})\ m$ of the galaxy is divided into (1) a hot phase with mass m_{h} at the virial temperature $T = (1/2)\ \mu\ m_{\mathrm{H}} v^2/k$ (m_{H} is the proton mass and μ is the mean molecular weight), (2) a cold phase with mass m_{c} able to cool radiatively within the galaxy survival time, and (3) the stars (with total mass m_*) forming from the cold phase on a time-scale τ_*. Initially, all baryons are assigned to the hot phase.

Also in this case, we compute galaxy spectra and luminosities by means of the spectrophotometric code developed by BC. The integrated stellar emission $S_\lambda(v,t)$ at the wavelength λ for a galaxy of circular velocity v at the time t is computed by convolving with the spectral energy distribution ϕ_λ obtained from population synthesis models:

$$S_\lambda(v,t) = \int_0^t \mathrm{d}t'\,\phi_\lambda(t-t')\,\dot{m}_*(v,t'). \tag{14}$$

ϕ_λ is taken from BC, with a Salpeter IMF. The metallicity is calculated by assuming a constant effective yield. The average galaxy metallicity varies between $Z \sim 0.003$ and $Z \sim 0.01$, in agreement with results of other SAMs (e.g. Cole et al. 2000). To calculate galactic spectra, we use simple stellar populations (SSPs) at fixed metallicity $Z = 0.004$. The use of the SSPs at $Z = 0.008$ would produce very small variations in our results, certainly negligible with respect to the observational errors.

The dust extinction affecting the above luminosities is computed assuming the dust optical depth to be proportional to the metallicity Z_{cold} of the cold phase and to the disc surface density, so that for the V band $\tau_V \propto m_{\mathrm{c}} Z_{\mathrm{cold}}/\pi\ r_{\mathrm{d}}^2$, where τ_v is the dust optical depth in the V band, m_{c} is the mass of the gas in the cold phase and r_{d} is the radius of the rotationally supported disc (see Menci et al. 2002). The proportionality constant is taken as a free parameter chosen to fit the bright end of the local LF. This fact yields, for the proportionality constant, the value 3.5 $\mathrm{M}_\odot^{-1}$ pc^2 with the stellar yield producing a solar metallicity for a $v = 220$ km s^{-1} galaxy. Physically, this recipe for computing dust extinction is identical to the one used for the PLE model (equation 6). To compute the extinction in the other bands, we use the extinction law of Calzetti (1997).

4 PLE VERSUS SAM: RESULTS

4.1 The SFR density

In Fig. 1, we show the evolution of the cosmic SFR density as a function of redshift as predicted in the framework of the two scenarios. The two curves have very different shapes: the PLE scenario predicts a peak at redshift $z \sim 5$ due to starbursts in spheroids (CM03), followed by a flat behaviour between $z \sim 4.2$ and $z \sim 3$ due to star formation in spiral galaxies. The maximum star formation in spirals cause a smaller peak of star formation at $z = 2$, and these galaxies are responsible for the decline of the SFR density between $z = 2$ and $z = 0$.

The hierarchical SAM by Menci et al. (2002) produces a curve characterized by a weak increase between $z = 5$ and $z \sim 3$, then becomes constant between $z \sim 3$ and $z \sim 2$ and finally starts to decrease at $z < 2$ down to $z = 0$. Between $z = 2$ and 0, the SAM predicts a higher amount of star formation than the PLE model.

4.2 The galaxy luminosity density

In Fig. 2, we show the redshift evolution of the LD in the rest-frame K (lower panel) and J (upper panel) bands, as predicted by the PLE model (solid lines) and by the SAM (dashed lines), compared with a set of observational data by various authors.

The K band, centred at $\lambda = 2.2$ μm, is dominated by long-lived, low-mass stars. The light emitted in this band is unaffected by dust extinction. At $z > 2$, the two curves have dramatically different

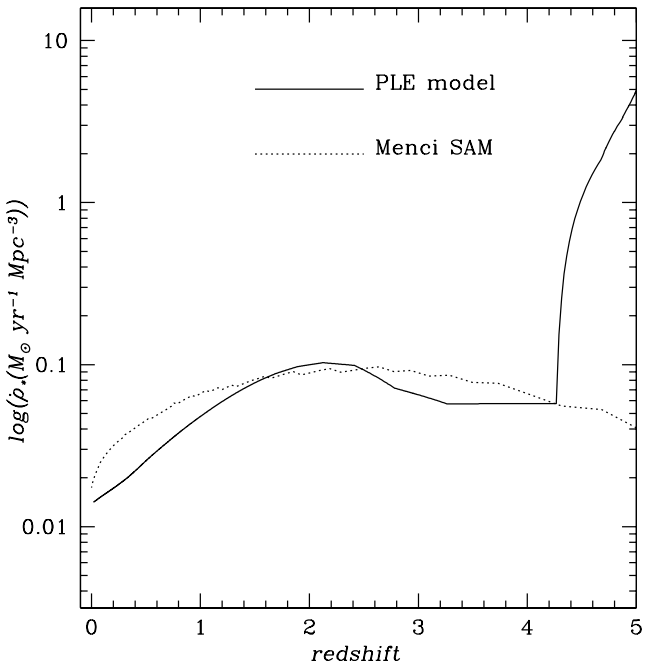

Figure 1. The global SFR density versus redshift as predicted by the PLE model (solid line) and by the hierarchical SAM (dotted line) of Menci et al. (2002).

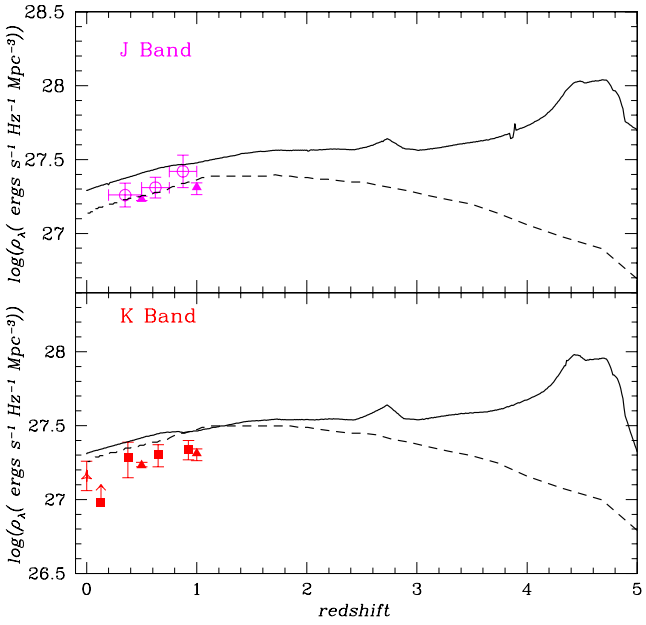

Figure 2. LD evolution in the rest-frame J (upper panel) and K (lower panel) bands as predicted by the PLE model by CM03 (solid curves) and by the hierarchical SAM of galaxy formation by Menci et al. (2002, dashed curves), and as observed by Lilly et al. (1996, open circles), Pozzetti et al. (2003, solid triangles), Gardner et al. (1997, three-pointed stars) and Cohen (2002, solid squares).

behaviours: the PLE curve shows a peak due to ellipticals, whereas the SAM curve has a broad peak centred at $z \sim 2$. On the other hand, it is compelling how similar the curves are at $z < 2$. At $z \leqslant 1$ we show the observational data by Pozzetti et al. (2003) and Cohen (2002), in substantial agreement with one another. In this redshift range, both curves show broadly a good agreement with the observational data.

The PLE scenario predicts a slightly higher LD at $z = 0$, mainly due to the higher number of old stars (hence redder galaxy colours) than the hierarchical picture. From the current set of observational data in the K band, it is practically impossible to distinguish between the two opposite galaxy formation scenarios. Rest-frame near-infrared deep galaxy surveys aimed at detecting faint sources, possibly located at high redshift, could provide us with fundamental hints to disentangle the PLE and hierarchical scenarios. In fact, if there were an epoch when the bulk of spheroidal galaxies was forming, the K-band LD would show a peak centred at the redshift corresponding to that epoch. On the other hand, if massive galaxy formation is distributed throughout an extended period, no peak in the K-band LD should be visible at high redshift. These results indicate that the study of the evolution of the K-band LD at redshift larger than 2 could represent the most direct observational strategy to establish the best scenario of galaxy formation.

Similar conclusions can be drawn in the J band, dominated both by relatively old stars experiencing the red giant branch phase and by young main-sequence stars, and in very similar fractions (Bruzual 2003).

The above results, concerning the LD in bands where the contribution of long-lived stars is relevant, show that the PLE model and SAM correctly predict the total amount of stars formed by $z \approx 0$, a conclusion confirmed by our analysis of the stellar mass density (see below, Section 4.3). The difference between the two scenarios is related to the rate of star formation during the cosmic time, which is better probed in the UV and B bands, where the contribution from massive, young stars is dominant.

Fig. 3 shows the evolution of the rest-frame UV and B LD, as predicted by the PLE model (solid curves) and SAM (dashed curves). In this case, the theoretical LDs have been calculated at 1400 Å and have been compared with data measured at various wavelengths, ranging from 1500 to 2800 Å (see caption to Fig. 3 for further details). In the two upper panels, the theoretical predictions are not corrected for dust extinction, whereas in the two lower panels the curves also take into account corrections for dust extinction. Looking at the upper left-hand panel it is possible to see how, once dust correction is not taken into account, in the UV band the PLE scenario predicts a strong peak at redshift 5. This peak is due to star formation in spheroids, which is absent in the hierarchical scenario of Menci et al. (2002). On the other hand, the SAM curve shows a broad peak, centred at redshift ~ 2.5. Another difference concerns the predicted evolution at redshift <1, where the curve from the SAM is constantly higher than the PLE one. This reflects the fact that the SAM predicts a higher amount of star formation occurring at $z < 1$ than the PLE curve; this is mainly due to the contribution of low-mass galaxies, which retain a relevant fraction of their gas down to small z, while the massive galaxy population, originated from clumps formed at high z in high-density regions, has already consumed most of the available cold gas reservoir.

The curves calculated in the B band (upper right-hand panel) show a behaviour very similar to that in the UV band, since both are dominated by the same types of stars, i.e. the youngest and the most massive ones. Both bands are sensitive to dust extinction, but in a different way: a comparison with the observations can be discussed only after having corrected the curves for dust obscuration.

In the lower left-hand panel of Fig. 3, the predicted UV luminosity densities have been corrected for dust extinction. A very important result regarding the UV LD predicted by the PLE scenario is that, once dust effects are properly taken into account, the peak at $z \sim 5$ due to ellipticals appears considerably reduced, with the PLE curve

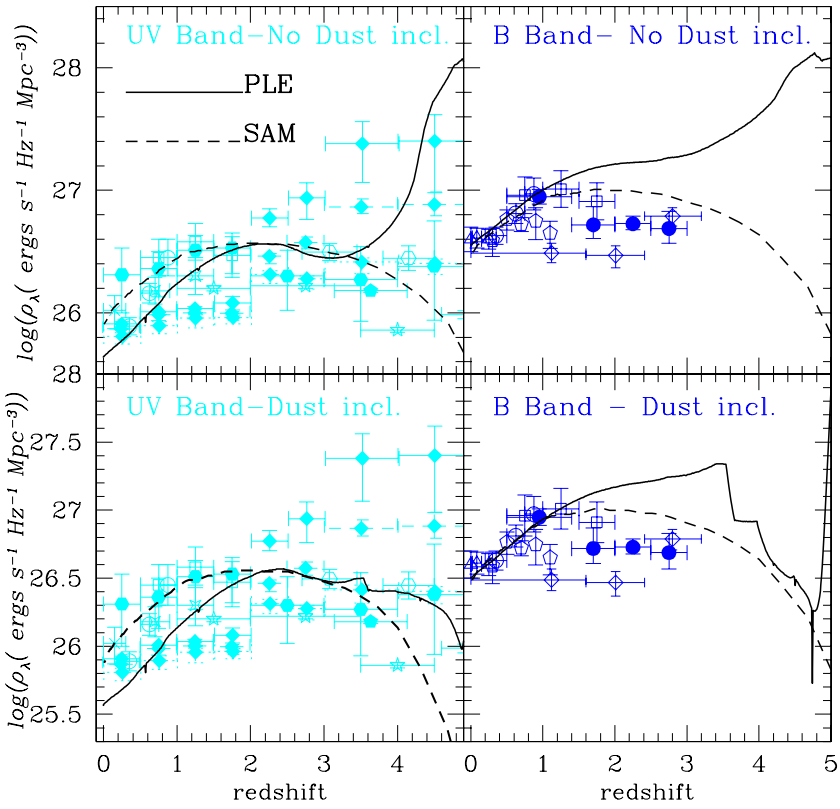

Figure 3. LD evolution in the rest-frame UV and *B* bands as predicted by our PLE models (solid curves) and by the hierarchical SAM of galaxy formation by Menci et al. (2002) (dashed curves), and as observed by various authors. For the UV band, the theoretical curves have been calculated at rest-frame 1400 Å. UV-band observations: Cowie, Songaila & Barger (1999, 2500 Å, four-pointed stars), Pascarelle et al. (1998, 1500 Å, solid hexagons), Steidel et al. (1999, 1500 Å, open hexagons), Treyer et al. (1998, 2000 Å, cross), Massarotti, Iovino & Buzzoni (2001, 1500 Å, five-pointed stars), Giavalisco et al. (2004, 1500 Å, solid pentagons), Lilly et al. (1996, 2800 Å, open circles), Connolly et al. (1997, 2800 Å, open squares) and Lanzetta et al. (2002, 1500 Å, solid diamonds, plotted for different values of the parameters involved in their measurement). *B*-band observations: Ellis et al. (1996, 4400 Å, open triangles), Dickinson et al. (2003, 4500 Å, solid circles), Rudnick et al. (2003, 4400 Å, open diamonds), Connolly et al. (1997, 4400 Å, open squares), Lilly et al. (1996, 4400 Å, open circles) and Wolf et al. (2003, 4560 Å, open pentagons). In the two upper panels, the theoretical curves are not corrected for dust extinction. In the two lower panels, the curves take into account dust extinction corrections.

showing a flat behaviour as in the observational data by Pascarelle, Lanzetta & Fernández-Soto (1998) and Steidel et al. (1999). This means that, as suggested by CM03, if the bulk of the star formation in the high-redshift Universe occurred in sites highly obscured by dust, most of it would be invisible for rest-frame UV surveys (see also Franx et al. 2003). Of great interest would be the study of the infrared/submillimetre LD, which would be considerably enhanced by the re-emission by dust of all the UV absorbed flux, and which is deferred to a forthcoming paper. It is also important to note that at redshift >4, the dust-corrected prediction from the hierarchical model is critical: at very high redshift, the unobscured UV LD (and hence the amount of star formation) is probably underestimated by the SAM by a factor of 3 or more, although the scatter in the data is too large to draw firm conclusions. However, recent independent analyses (Fontana et al. 2003a; Menci et al. 2004) have shown that when only the bright galaxy population is selected, the paucity of the predicted UV LD compared with observations is more clearly revealed, confirming that at those z some fundamental process must be at work, such as bursts of star formation with a rate higher than that predicted by standard SAMs. Such a process could be constituted by starbursts triggered by interactions of galaxies, as described in Menci et al. (2004) but not included in the SAM adopted in this paper. These starbursts would speed up the formation of stars in massive galaxies preferentially at high z (where the density of galaxies is larger). Such starbursts would affect mainly the massive galaxies (because of their larger cross-section for interactions) and would hence constitute the counterpart of the spheroids assumed to form at high redshift in the PLE model.

Of particular interest are the data of Lanzetta et al. (2002, solid diamonds in Fig. 3), who found a monotonically increasing behaviour up to redshift 10. These data also take into account surface brightness dimming effects, which are likely to be serious at high redshift and which have never been considered before by any other group. In their most extreme case, the observations are as high as the values predicted by the PLE curve uncorrected for dust. If confirmed by other deep surveys, the data by Lanzetta et al. (2002) could represent the most direct evidence in favour of a peak of star formation at high redshift. If true, such a peak would be problematic to explain for both PLE and hierarchical scenarios. However, it is also worth stressing that among the three sets of data calculated by Lanzetta et al. (2002), the favoured one by the authors is represented by the solid diamonds with dotted error bars, of which the point at redshift $z > 4$ is in very good agreement with the PLE predictions but discordant with the SAM predictions.

Also in the case of the high-redshift UV LD, the PLE and the hierarchical model used in the present work produce very different predictions, and the observations clearly allow us to discriminate between the two.

Different indications seem to come from the UV LD at $z < 1$. The prediction from the SAM by Menci et al. (2002) can nicely reproduce the data, whereas the PLE prediction is lower than the observations. At $z = 0.2$, where the lowest redshift observations have been performed by Treyer et al. (1998) at $\lambda = 2000$ Å, the PLE models underestimates the data by a factor of ∼2.2, whereas the data by Lanzetta et al. (2002) at $z = 0.25$ are underestimated by a factor of ∼1.2. The explanation of this discrepancy is in part related to the fact that in the morphological classification of the PLE scenario we do not take into account nearby starburst galaxies, which can contribute up to ∼ 20 per cent of the global star formation in the local Universe (Brinchmann et al. 2004). This would be enough to account for the discrepancy between the PLE predictions and the data by Lanzetta et al. (2002), but not for the data by Treyer et al. (1998).

However, beside the missing contribution by starbursts, the uncertainty in the *B*-band LF normalization also plays an important role. The local *B*-band LD adopted here for the PLE model is the one measured by Marzke et al. (1998), whose normalization is the lowest among the values provided by the most popular surveys (see Cross et al. 2001) and whose uncertainty could reach also factors of ∼2. This fact could lead to a slight underestimation of all the LD values predicted by the PLE model.

The lower right-hand panel of Fig. 3 shows the observed evolution of the *B*-band LD compared with the predictions corrected for dust extinction. At $z < 2$ the PLE and SAM curves are overlapping and both are in excellent agreement with the observations. At $z > 2$, the only available measures are the ones by Dickinson et al. (2003) and by Rudnick et al. (2003), none of which is accurately reproduced by any of these scenarios. In this case, however, the discrepancy is more critical for the PLE model than for the SAM. It is worth stressing that the combination of small field, cosmic variance effects, dust extinction and incompleteness is a non-negligible source of uncertainty in the data. Indeed, some of these effects also cause an underabundance of massive galaxies as obtained by Dickinson et al. (2003) and a consequent underestimation of the stellar mass density with respect to the estimates by other authors (Fontana et al. 2003b, see also Section 4.4). Also in the *B* band, absorption by dust significantly reduces the peak at z ∼4–5 due to ellipticals, although to a lesser extent than in the case of the UV band. In particular, the PLE model predicts a very narrow peak between redshifts 5 and 4.8, corresponding to a time interval of ∼ 60 Myr. During this interval, the gas in spheroids is experiencing strong metal enrichment; consequently its optical depth is progressively rising to its maximum (see equation 6) and the *B*-band LD to its minimum. The fact that the peak is so narrow is due to the assumption that all spheroids start forming stars at the same redshift ($z_f = 5$) and the star formation is completed after $t \simeq 0.3$ Gyr. In a more realistic picture, the first galaxies started forming stars before redshift 5 (see Giavalisco et al. 2004) and in a finite redshift range, so that the very narrow peak would become larger and lower. Objects at high redshift which could be associated with a tail in the formation of galactic spheroids are the Lyman-break galaxies, which are usually detected at $z \geqslant 3$ and which show a large range of stellar population ages (Papovich, Dickinson & Ferguson 2001; Shapley et al. 2001). In our picture, these galaxies can be associated with forming spheroids (see Matteucci & Pipino 2002), with total stellar masses of the order of that of the Galactic bulge. Other interesting objects are the submillimetre-bright galaxies, detected at z ∼2–3 and characterized by star formation rates of the order of 100–1000 $M_\odot$ yr^{-1} (Smail et al. 2004). These galaxies have typical space densities of $\sim 10^{-4}$ Mpc^{-3}, i.e. comparable to L_* ellipticals (Blain et al. 2004). They appear as massive as the largest spheroids observed locally and gas-rich (see Neri et al. 2003), and in the PLE picture they can be associated with a tail in the formation of massive spheroids. In a ΛCDM cosmology, the time lag between redshifts 2 and 5 corresponds to ∼2.3 Gyr. This time-spread is consistent with what is suggested by Bower et al. (1992), who found that in galaxy clusters the redshift range of interest for major spheroid formation could correspond to an age spread of $\Delta_{\rm form} \sim 2$ Gyr. In the field, Bernardi et al. (1998) found a slightly larger age spread for large spheroids, i.e. $\Delta_{\rm form} \sim 3$ Gyr.

Another peak is predicted by the PLE curve at $z \sim 3.5$, once the interstellar gas has completely been ejected by spheroids into the IGM, making the emission by stars visible.

Further observations in the *B* band at redshifts of 2–3 and beyond, within the reach of next-generation deep galaxy surveys, could constitute a stringent test for PLE models. If the behaviour shown by the present data should be confirmed by future surveys, this could constitute strong evidence for galaxy density evolution, the process not taken into account in PLE models.

4.3 The comoving galaxy number density

In Fig. 4 we plot the redshift evolution of the number density of bright galaxies. Such a quantity is obtained by integrating the rest-frame luminosity function at 1500 Å, considering only the objects brighter than the apparent magnitude limit of $m_{1500} = 25.5$. We consider only the redshift range between $z = 2$ and 5, i.e. the interval where the predictions provided by the PLE and hierarchical scenarios differ most. The observational data belong to various authors (see caption to Fig. 4 for further details) and have all been taken

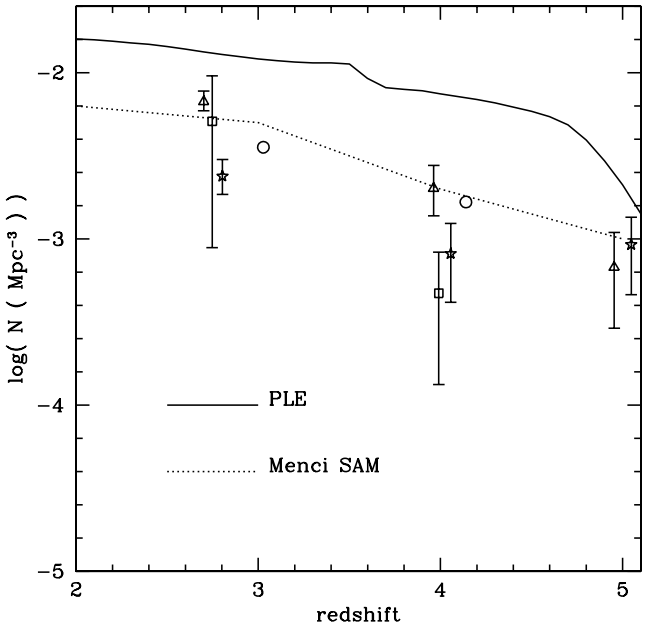

Figure 4. Evolution of the total comoving number density of galaxies brighter than 25.5 at rest-frame 1500 Åbetween redshifts 2 and 4.9, as predicted by by the PLE model (solid line) and by the hierarchical SAM of galaxy formation by Menci et al. (2002) (dotted line), and as observed by Steidel et al. (1999, open circles), Pozzetti et al. (1998, open squares), Lanzetta et al. (1999, open triangles) and Chen et al. (1998, stars). This compilation of data has been taken from Somerville et al. (2001). For the sake of consistency with the data, in this case we assume a ΛCDM cosmology with $H_0 = 70$ km s^{-1}Mpc^{-1}. The theoretical predictions have been corrected for dust extinction.

from Somerville et al. (2001). The observations indicate that most of the galaxy number evolution occurs in this redshift range: the number of bright galaxies is increasing by a factor of ~ 6 between redshift $z = 5$ and $z \sim 2.8$. The theoretical curves plotted in Fig. 4 take into account dust corrections and represent the predictions according to the PLE (solid line) and hierarchical (dotted line) scenarios. The comparison between the theoretical predictions and the observations considered in this case indicates that the PLE scenario is inadequate to describe the number evolution of bright UV galaxies, since it systematically overestimates the observed number at all redshifts. We note that the disagreement between the PLE curve and the data is a maximum at redshift $z \sim 4$, where the discrepancy is a factor of $\sim$5. On the other hand, the hierarchical scenario described by the SAM allows us to reproduce the observed trend with very good accuracy. It is worth noting that the study of the number density of bright UV galaxies represents an interesting test for the evolution of star-forming galaxies at high redshift but, like the UV LD, it does not provide any information about the formation of massive spheroids, which most likely occurs in dust-enshrouded environments so they are invisible in the rest-frame UV. Furthermore, if at redshift 3–4 there were already a significant number of massive galaxies containing old stars, generating red spectra, such a population would certainly be missed by UV galaxy surveys. A fruitful test for the identification of the number of massive galaxies at high redshift is the study of the evolution of the stellar mass density.

4.4 The evolution of the stellar mass density

Fig. 5 shows the redshift evolution of the stellar mass fraction as predicted by the PLE model (solid line) and by the SAM (dotted line). Each curve is normalized to the value for the stellar mass density predicted at the present day. This figure is helpful for understanding what percentage of the present-day stellar mass is in place at any given redshift according to the predictions of the two scenarios. The two curves have very different behaviours: according to the PLE model, nearly half of the stars observable today are already in place at $z \sim 4$, corresponding to 1.63 Gyr after the big bang for the cosmology adopted here. This is due to the stellar mass produced in spheroids. The increase from $z = 4$ to 0 is due to quiescent star formation in spirals (CM03). At $z = 1$, corresponding to an age of the Universe of 6.2 Gyr, the PLE model predicts that 85 per cent of the present stellar mass is already in place.

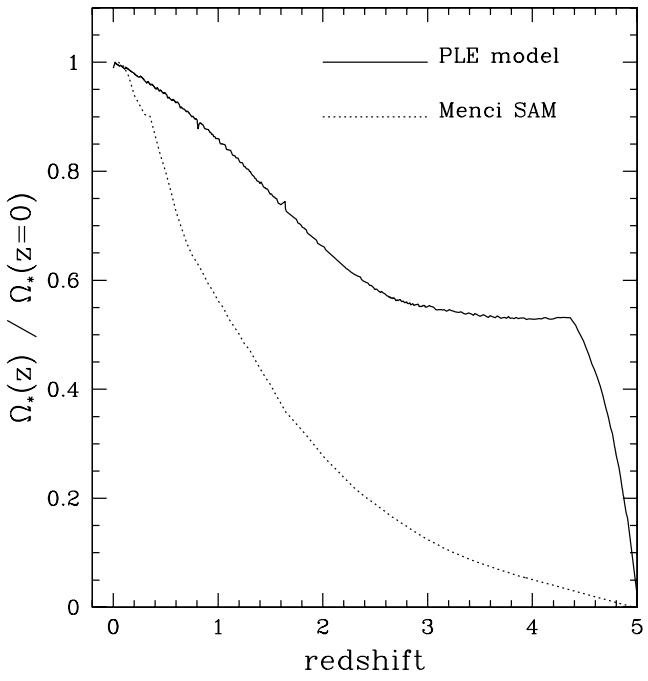

Figure 5. Predicted fraction of the total present-day stellar mass as a function of redshift. Solid line: PLE model. Dotted line: SAM by Menci et al. (2002).

According to the hierarchical SAM, the build-up of the stellar mass occurs progressively, with half of the total stellar mass in place at $z \sim 1.2$, i.e. 5.42 Gyr after the big bang. By $z \sim 1$, the SAM predicts that nearly 60 per cent of the total present stellar mass is present.

Fig. 6 shows a comparison between the stellar mass density as observed by various authors and as predicted by PLE models and by the SAM. This comparison demonstrates that, owing to the extreme differences between the PLE and SAM predictions, the observation of the stellar mass density constitutes another very helpful strategy to distinguish between the PLE and the hierarchical scenario.

In the upper panel of Fig. 6, we show the evolution of the stellar mass density by considering galaxies of all masses, namely no mass cut-off has been applied to the predicted values. The theoretical predictions are compared with observational estimates by various authors (for further details, see caption of Fig. 6) In general, the main sources of uncertainties in the data are dust extinction and cosmic variance effects due to the small field. The data by Fontana et al. (2003b) are taken from a large volume and are corrected for dust extinction. However, as emphasized by the authors, they may still suffer for incompleteness at the bright end of the mass function. To estimate to what extent these effects could alter the real values is difficult: for instance, the amounts of dust can vary considerably from one galaxy to another. Also the cosmic variance effects are in principle difficult to evaluate. It is worth noting that all these effects conspire to lower the estimates of the stellar mass at redshifts larger than 1: for these reasons, it is safe to consider the data as lower limits. The PLE and SAM curves are both in reasonable agreement with the data within redshift $z < 1.5$. At redshifts higher than 1.5, if we consider the predicted total stellar mass the PLE model presents a noticeable discrepancy with the observations: if we consider the central values estimated by Fontana et al. (2003b), the discrepancies between observations and PLE predictions are by factors of 3–6. On the other hand, on average, the SAM predictions seem to show a good agreement with the observed values.

In the lower panel of Fig. 6, we show the predicted evolution of the stellar mass density according to the PLE (solid curves) and SAM (dotted curves) and by considering all the stars in galaxies with masses above three mass cut-offs, namely $M > 10^{10.2}$ $M_\odot$ (thick green lines in online version of article), $M > 10^{10.5}$ $M_\odot$ (thick red lines in online version) and $M > 10^{10.8}$ $M_\odot$ (thick black lines in online version). Such predictions are compared with observational values obtained by Glazebrook et al. (2004) with the same criteria, i.e. by applying the same three mass cut-offs to the data sample. The values by Glazebrook et al. (2004), corresponding to the three cut-offs, are plotted with the same colour as used for the theoretical predictions. The adoption of the mass cut-offs is very helpful in establishing a full correspondence between observations and theoretical predictions, and to have a very clear picture of the number of massive galaxies that the PLE and hierarchical scenarios predict at any redshift, respectively. For the theoretical predictions, the threshold values are the same as adopted by Glazebrook et al. (2004) and are used as indicative values. Adopting different IMF

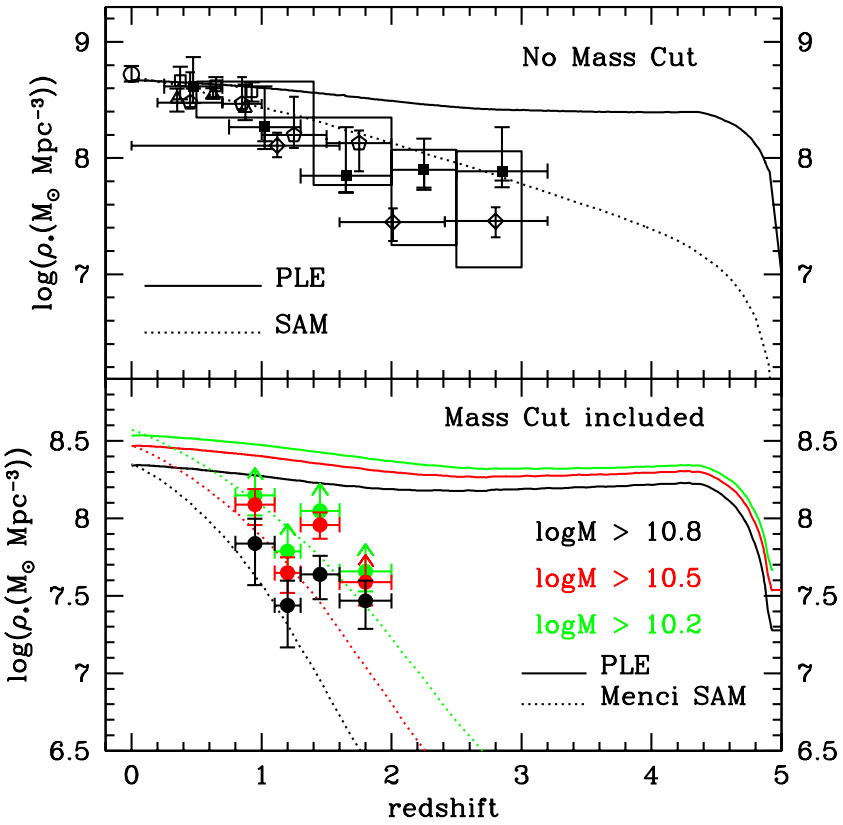

Figure 6. Upper panel: evolution of the stellar mass density as predicted by our PLE models (solid line), by the hierarchical SAM of galaxy formation by Menci et al. (2002) and as observed by various authors: Dickinson et al. (2003, large rectangles), Cole et al. (2001, open circle), Brinchmann & Ellis (2000, open triangles), Cohen (2002, open squares), Fontana et al. (2003b, solid squares), Rudnick et al. (2003, open diamonds) and Fontana et al. (2004, open pentagons). No mass cut-off has been applied to the predicted values. Lower panel: the three solid (dotted) lines with increasing thickness represent the predicted evolution of the stellar mass density according to the PLE (SAM) scenario by considering all the stars in galaxies with masses above three mass cut-offs, namely $M > 10^{10.2}$ $M_{\odot}$, $M > 10^{10.5}$ $M_{\odot}$ and $M > 10^{10.8}$ $M_{\odot}$. The predictions are compared with observational values obtained by Glazebrook et al. (2004, solid circles) with the same criteria, i.e. by applying the same three mass cut-offs to the data sample. The values by Glazebrook et al. corresponding to the three cut-offs are plotted with the same colours as used for the theoretical predictions.

results in different values of the thresholds (a factor of 1.82 higher in the case of a Salpeter IMF). Such variations translate into small differences in the theoretical stellar mass densities, which do not alter our conclusions. If we compare the PLE predictions with the data calculated with the three cut-offs, we notice that the agreement between data and predictions does not improve and that the PLE model in general tends to overestimate the stellar mass density in massive galaxies, in particular at redshifts $z > 1$.

If we compare the SAM predictions with the data, we notice that the hierarchical picture can reproduce the observed data with the three cut-offs up to redshift $z \sim 1.2$, whereas at higher redshift it tends to underestimate the observations. The disagreement is particularly strong for the highest mass cut-off ($M > 10^{10.8}$ $M_{\odot}$). This shows that at redshifts $z \geqslant 1$, according to the SAM predictions, the bulk of the stellar mass resides in objects with masses $M < 10^{10.2}$ $M_{\odot}$. These small objects would be too faint to be visible by any current high-redshift survey. Also in this case, this problem is alleviated by considering the effect of interaction-driven starbursts in massive galaxies at high-redshift (see Menci et al. 2004), which would increase the fraction of stellar mass already in place at $z = 2$ to a value around 0.3 of the present mass density.

It is very interesting to see how, by means of ΛCDM cosmological numerical simulations, Nagamine et al. (2004) find a strong discrepancy between the predicted and observed amount of stellar mass at redshift $z > 1.5$. Their simulations indicate an excess of stellar mass with respect to observational estimates at high redshift, in analogy with the result of the PLE model considered in this work. This is another indication suggesting that the global star formation of the Universe may have proceeded in the past at levels somewhat higher than predicted by semi-analytical models, and it confirms that effects such as dust obscuration and cosmic variance may still seriously prevent us from having a clear picture of galaxy evolution at redshifts $z > 1$.

Recently, the Great Observatories Origins Deep Survey has provided evidence for a population of galaxies showing distorted morphologies and with ongoing merger activity located at $z \geqslant 1.5$ (Somerville et al. 2004). The number density of such bright objects is underestimated by current hierarchical SAMs and overestimated by PLE models. To assess the role of such galaxies in the stellar and metal budget would be of primary interest in order to have further crucial hints on the evolution of galaxies at redshifts larger than 1.

5 CONCLUSIONS

In this paper we have studied the evolution of the cosmic star formation, the galaxy LD and the stellar mass density by means of two opposite galaxy evolution pictures: the pure luminosity

evolution model developed by CM03 and the semi-analytical model of hierarchical galaxy formation by Menci et al. (2002). The former predicts a peak at redshift $z = 5$, due to intense star formation in ellipticals, followed by a phase of quiescent and continuous star formation occurring in spiral galaxies. The SAM predicts a smoother behaviour, following the gradual build-up of galactic DM haloes through repeated merging events. The aim was to derive constraints on the relative importance of different physical processes – like the dependence on morphology of the star formation history, the density evolution of the galaxy population, the impulsive starbursts – in determining the observed properties of the galaxies.

We have shown that the evolution of the cosmic SFR density in the two models behaves quite differently. However, the integrals of the cosmic SFR at redshift $z \leqslant 1$, probed by the stellar mass density evolution in this redshift range, are in good agreement. This ensures that the total amounts of stars formed along the star formation histories are similar (and in agreement with the observations). To probe the rate of star formation at different cosmic epochs we investigated the LD in the UV and *B* bands, where the emission is dominated by young, short-lived massive stars. The comparison with the *available* data shows the following.

(1) At redshift $z > 4$, the SAM tends to underestimate the observed UV LD which, as several current surveys indicate, is a non-decreasing function of z. On the other hand, the PLE predictions can account fairly well for such an observed trend. If future surveys confirm such behaviour, this could indicate that some fundamental processes should be inserted into the SAM to boost the star formation at high redshifts. An example of such a process could be the interaction-driven starbursts suggested by Menci et al. (2004).

(2) In the *B* band the PLE model tends to overestimate the observed LD at $z > 2.5$ by a factor increasing with z. This is the consequence of placing a rapid formation of all the elliptical galaxies at $z \approx 5$. While dust extinction and incompleteness severely affect the comparison with present data, if future observations do not indicate a substantial growth of the *B*-band luminosity density for $z \geqslant 2.5$–3, this would point toward a galaxy density evolution, the main process not included in PLE models.

(3) At low redshift ($z < 1$), the local UV LD predicted by the SAM is about a factor of 2 larger than those arising from PLE models. This is because in hierarchical scenarios at low redshift the low-mass galaxies still retain a significant fraction of their cold gas reservoirs, while the massive ones have already exhausted most of their fuel at high redshift, since the latter are formed from clumps originating in biased high-density regions of the cosmic density field. In hierarchical models, at low z the contribution of low-mass galaxies sustains the global SFR above the value obtained in the continuous, passive-evolution PLE models. The above discussion shows that, while the local *J* and *K* observations will hardly contribute to discriminating between the two scenarios, accurate measurements of the local UV LD would be effective in constraining the models.

(4) The observed evolution of the comoving number density of bright galaxies at redshift $z \geqslant 3$ is well reproduced by the hierarchical SAM, whereas, for the set of data considered here, the PLE model overestimates the observed densities by factors between 2 and 5.

(5) The stellar mass density constitutes a complementary probe for the PLE and hierarchical scenarios. In general, both the PLE and hierarchical predictions allow us to reproduce the observed stellar mass density evolution up to $z = 1$. At $z > 1$, the predicted stellar mass densities diverge, with the PLE predictions remaining almost constant up to redshift $z \approx 4$ and the SAM predictions continuously dropping with increasing z. Without any mass cut-off on the theoretical predictions, the PLE model overestimates the data by factors of 3–6. If we calculate the stellar mass density evolution and apply the three mass cut-offs, as performed by Glazebrook et al. (2004), in general the discrepancies between the PLE model and the observations at $z > 1$ do not reduce. On the other hand, the hierarchical picture underestimates the observations for all three values of the mass cut-offs at redshifts $z > 1.2$. This is related to the fact that, at redshifts $z \geqslant 1$, according to the SAM predictions the bulk of the stellar mass resides in objects with masses $M < 10^{10.2}\ \mathrm{M}_{\odot}$. These small objects would be too faint to be visible by any current high-redshift survey. Also in this case, the discrepancy between the hierarchical model and observations is partially alleviated by introducing a population of high-redshift starbursts in massive galaxies (Menci et al. 2004), which would bring the mass density at $z = 2$ to values around $1/3$ of the local value, in much better agreement with the data but still well below the PLE predictions. Thus, in principle, more precise observations of the stellar mass density at $z > 2$ will be able to discriminate between the PLE models and the SAM including starbursts at high z. On the other hand, some indications against hierarchical formation of elliptical galaxies are provided by chemical constraints, in particular the increase of the [Mg/Fe] ratio with galaxy luminosity (Thomas 1999; Pipino & Matteucci 2004). This fact indicates that the most massive ellipticals stopped forming stars before the less massive ones. All of these facts together will have to be taken into account eventually before drawing firm conclusions.

As forthcoming work, to investigate star and massive galaxy formation at high redshift we will use other diagnostics, such as infrared and submillimetre emission.

ACKNOWLEDGMENTS

We thank an anonymous referee for several enlightening suggestions which improved the quality of this work. We thank Daniela Calzetti for many useful suggestions on the treatment of dust extinction, and Cristina Chiappini and Paolo Tozzi for careful readings of the manuscript and for several useful comments. FC and FM also acknowledge funds from MIUR, COFIN 2003, prot. N. 2003028039.

REFERENCES

Arimoto N., Yoshii Y., 1987, A&A, 173, 23
Barger A. J., Cowie L. L., Trentham N., Fulton E., Hu E. M., Songaila A., Hall D., 1999, AJ, 117, 102
Baugh C. M., Cole S., Frenk C. S., Lacey C. G., 1998, ApJ, 498, 504
Bernardi M., Renzini A., da Costa L. N., Wegner G., Alonso M. V., Pellegrini P. S., Rité C., Willmer C. N. A., 1998, ApJ, 508, L43
Binney J., Merrifield M., 1998, Galactic Astronomy. Princeton Univ. Press, Princeton, NJ
Blain A. W., Chapman S. S., Smail I., Ivison R., 2004, ApJ, in press (astro-ph/0405035)
Bond J. R., Cole S., Efstathiou G., Kaiser N., 1991, ApJ, 379, 440
Bower R. G., 1991, MNRAS, 248, 332
Bower R. G., Lucey J. R., Ellis R. S., 1992, MNRAS, 254, 613
Bradamante F., Matteucci F., D'Ercole A., 1998, A&A, 337, 338
Brinchmann J., Ellis R. S., 2000, ApJ, 536, 77
Brinchmann J., Charlot S., White S. D. M., Tremonti C., Kauffmann G., Heckman T., Brinkmann J., 2004, MNRAS, 1151, 1179
Bruzual A. G., 2003, in Pérez-Fournon I., Balcells M., Moreno-Inserlis F., Sánchez F., eds, XI Canary Islands Winter School of Astrophysics, Galaxies at High Redshift. Cambridge University Press, Cambridge, p. 185

Bruzual A. G., Charlot S., 2003, MNRAS, 344, 1000
Bundy K., Fukugita M., Ellis R. S., Kodama T., Conselice C. J., 2004, ApJ, 601, L123
Calura F., 2004, PhD thesis, Trieste University
Calura F., Matteucci F., 2003, ApJ, 596, 734 (CM03)
Calura F., Matteucci F., 2004, MNRAS, 350, 351
Calzetti D., 1997, in Waller W. H., Fanelli M. N., Hollis J. E., Danks A. C., eds, AIP Conf. Proc. Vol. 408, The Ultraviolet Universe at Low and High Redshift: Probing the Progress of Galaxy Evolution. Am. Inst. Phys., New York, p. 403
Calzetti D., 2001, PASP, 113, 1449
Calzetti D., Kinney A. L., Storchi-Bergmann T., 1994, ApJ, 429, 582
Chen H.-S., Fernandez-Soto A., Lanzetta K. M., Pascarelle S. M., Puetter, R. C., Yahata N., Yahil A., 1998, preprint (astro-ph/9812339)
Chiappini C., Matteucci F., Gratton R., 1997, ApJ, 477, 765
Chiappini C., Matteucci F., Romano D., 2001, ApJ, 554, 1044
Cohen J. G., 2002, ApJ, 567, 672
Cole S., Lacey C. G., Baugh C. M., Frenk C. S., 2000, MNRAS, 319, 168
Cole S. et al., 2001, MNRAS, 326, 255
Connolly A. J., Szalay A. S., Dickinson M. E., SubbaRao M. U., Brunner R. J., 1997, ApJ, 486, L11
Conselice C. J., Bershady M. A., Dickinson M., Papovich C., 2003, AJ, 126, 1183
Cowie L., Songaila A., Barger A., 1999, AJ, 118, 603
Cross N. et al., 2001, MNRAS, 324, 825
Dickinson M., Papovich C., Ferguson H. C., Baudavári T., 2003, ApJ, 587, 25
Djorgovski S., Davis M., 1987, ApJ, 313, 59
Ellis R. S., Colless M., Broadhurst T., Heyl J., Glazebrook K., 1996, MNRAS, 280, 235
Fontana A., Poli F., Menci N., Nonino M., Giallongo E., Cristiani S., D'Odorico S., 2003a, ApJ, 587, 544
Fontana A. et al., 2003b, ApJ, 594, L9
Fontana A. et al., 2004, A&A, in press (astro-ph/0405055)
Franceschini A., Silva L., Fasano G., Granato L., Bressan A., Arnouts S., Danese L., 1998, ApJ, 506, 600
Franx M. et al., 2003, ApJ, 587, L79
Gardner J. P., Sharples R. M., Frenk C. S., Carrasco B. E., 1997, ApJ, 480, L99
Giavalisco M. et al., 2004, ApJ, 600, L103
Glazebrook K. et al., 2004, Nat, in press (astro-ph/0401037)
Im M., Griffiths R. E., Ratnatuga K. U., Sarajedini V. L., 1996, ApJ, L79
Im M. et al., 2002, ApJ, 571, 136
Kauffmann G., White S. D. M., Guiderdoni B., 1993, MNRAS, 264, 201
Kauffmann G., Charlot S., White S., 1996, MNRAS, 283, 117
Kennicutt R. C., 1998, ApJ, 498, 541
Kochanek C. S. et al., 2000, ApJ, 543, 131
Kodama T., Bower R. G., Bell E. F., 1999, MNRAS, 306, 561
Lacey C., Cole S., 1993, MNRAS, 262, 627
Lanzetta K. M., Chen H.-S., Fernandez-Soto A., Pascarelle S., Puetter R., Yahata N., Yahil A., 1999, in Weymann R., Storrie-Lombardi L., Sawicki M., Brunner R., eds, ASP Conf. Proc., Vol. 191, Photometric Redshifts and High Redshift Galaxies, Astron. Soc. Pac., San Francisco, p. 223
Lanzetta K. M., Yahata N., Pascarelle S., Chen H., Fernández-Soto A., 2002, ApJ, 570, 492
Larson R. B., 1974, MNRAS, 166, 585
Le Févre O. et al., 2000, MNRAS, 311, 565
Lilly S. J., LeFévre O., Hammer F., Crampton D., 1996, ApJ, 460, L1
Lilly S. et al., 1998, ApJ, 500, 75
Marzke R. O., Nicolaci Da Costa L., Pelligrini P., Willmer C. N. A., Geller M., 1998, ApJ, 503, 617
Massarotti M., Iovino A., Buzzoni A., 2001, ApJ, 559, L105
Matteucci F., 1992, ApJ, 397, 32
Matteucci F., 1994, A&A, 288, 57
Matteucci F., François P., 1989, MNRAS, 239, 885
Matteucci F., Pipino A., 2002, ApJ, 569, L69
Matteucci F., Tornambé A., 1987, A&A, 185, 51
Menanteau F., Ellis R. S., Abraham R. G., Barger A. J., Cowie L. L., 1999, MNRAS, 309, 208
Menci N., Cavaliere A., Fontana A., Giallongo E., Poli F., 2002, ApJ, 575, 18
Menci N., Cavaliere A., Fontana A., Giallongo E., Poli F., Vittorini V., 2004, ApJ, 604, 12
Nagamine K., Cen R., Hernquist L., Ostriker J. P., Springel V., 2004, ApJ, in press (astro-ph/0311294)
Neri R. et al., 2003, ApJ, 597, L113
Nomoto K., Hashimoto M., Tsujimoto T., Thielemann F. K., Kishimoto N., Kubo Y., Nakasato N., 1997a, Nucl. Phys. A, 616, 79
Nomoto K., Hashimoto M., Tsujimoto T., Thielemann F.-K., Kishimoto N., Kubo Y., Nakasato N., 1997b, Nucl. Phys. A, 621, 467
Papovich C., Dickinson M., Ferguson H. C., 2001, ApJ, 559, 620
Pascarelle S. M., Lanzetta K. M., Fernández-Soto A., 1998, ApJ, 508, L1
Patton D. R., Pritchet C. J., Yee H. K. C., Ellingson E., Carlberg R. G., 1997, ApJ, 475, 29
Peebles P. J. E., 2002, in Metcalfe N., Shanks T., eds, ASP Conf. Ser., A New Era in Cosmology. Astron. Soc. Pac., San Francisco, Vol. 283, p. 351
Pipino A., Matteucci F., 2004, MNRAS, 347, 968
Poggianti B. M., 1997, A&AS, 122, 399
Poli F., Giallongo E., Menci N., D'Odorico S., Fontana A., 1999, ApJ, 527, 662
Pozzetti L., Madau P., Zamorani G., Ferguson H. C., Bruzual G. A., 1998, MNRAS, 298, 1133
Pozzetti L. et al., 2003, A&A, 402, 837
Press W. H., Schechter P., 1974, ApJ, 187, 425
Renzini A., 1999, in Carollo C. M., Ferguson H. C., Wyse R. F. G., eds, When and How do Bulges Form and Evolve? Cambridge Univ. Press, Cambridge, p. 9
Renzini A., Ciotti L., 1993, ApJ, 416, L49
Rudnick G. et al., 2003, ApJ, 599, 847
Rusin D. et al., 2003, ApJ, 587, 143
Salpeter E. E., 1955, ApJ, 121, 161
Sandage A., 1986, A&A, 161, 89
Scalo J. M., 1986, Fundam. Cosmic Phys., 11, 1
Schade D. et al., 1999, ApJ, 525, 31
Schechter P., 1976, ApJ, 203, 297
Schlegel D. J., Finkbeiner D. P., Davis M., 1998, ApJ, 500, 525
Seaton M. J., 1979, MNRAS, 187, 73
Shapley A. E., Steidel C. C., Adelberger K. L., Dickinson M., Giavalisco M., Pettini M., 2001, ApJ, 562, 95
Smail I., Chapman S., Blain A., Ivison R., 2004, in Colless M., Staveley-Smith L., eds, Proc. IAU Symp. 216, ASP Conf. Ser., Maps of the Cosmos, in press (astro-ph/0311285)
Somerville R. S., Primack J. R., Faber S. M., 2001, MNRAS, 320, 504
Somerville R. S. et al., 2004, ApJ, 600, L135
Springel V., Hernquist L., 2003, MNRAS, 339, 312
Steidel C. C., Adelberger K. L., Giavalisco M., Dickinson M., Pettini M., 1999, ApJ, 519, 1
Thomas D., 1999, MNRAS, 306, 655
Totani T., Yoshii Y., 2000, ApJ, 540, 81
Treyer M. A., Ellis R. S., Milliard B., Donas J., Bridges T. J., 1998, MNRAS, 300, 303
van Albada T. S., 1982, MNRAS, 201, 939
van den Hoeck L. B., Groenwegen M. A. T., 1997, A&AS, 123, 305
van Dokkum P. G., Ellis R. S., 2003, ApJ, 592, L53
van Dokkum P. G., Franx M., Fabricant D., Illingworth G. D., Kelson D. D., 2000, ApJ, 541, 95
van Dokkum P. G., Franx M., Kelson D. D., Illingworth G. D., 2001, ApJ, 553, L39
White S. D. M., Rees M. J., 1978, MNRAS, 183, 341
Wolf C., Meisenheimer K., Rix H.-W., Borch A., Dye S., Kleinheinrich M., 2003, A&A, 401, 73
Zepf S. E., 1997, Nat, 390, 377

This paper has been typeset from a TEX/LATEX file prepared by the author.